Journal of Applied Electrochemistry **34**: 533–543, 2004.

Effects of thiourea on anodic dissolution of Au and surface oxidation behaviour in aq $HClO_4$ studied by means of an EQCN

M. TIAN and B.E. CONWAY*
Chemistry Department, University of Ottawa, 10 Marie Curie Street, Ottawa, ON, K1N 6N5, Canada
*(*author for correspondence, fax: +1 613 5625170)*

Received 11 September 2003; accepted in revised form 26 November 2003

Key words: Au electrode, dissolution, electrochemical nanobalance, perchloric acid, rotating-disc electrode, thiourea

Abstract

Anodic dissolution of Au is facilitated by the presence of thiourea owing to formation of strongly complexed Au ions. The present paper reports studies of this process using cyclic voltammetry (CV), chronopotentiometry and chronoamperometry, usefully complemented by nanogravimetry employing an electrochemical quartz-crystal nanobalance (EQCN). The molar masses per faraday for Au dissolution were determined from EQCN measurements, coupled with information derived from CV, chronopotentiometry and chronoamperometry, and clearly indicate that Au becomes dissolved over the potential range 0.45–0.65 V vs RHE via a $1e^-$ oxidation process in 0.5 M $HClO_4$ solution containing thiourea. The peak potential for Au dissolution in the presence of thiourea is about 600 mV less positive than that in the presence of Br^- or Cl^- (1.20 V vs RHE for Br^- and 1.39 V vs RHE for Cl^-). The linear relationship between anodic peak currents at about 0.630 V vs RHE and square-root of the sweep rate indicates that the Au dissolution process is diffusion-controlled. The anodic current efficiency for Au dissolution is 93%.

1. Introduction

Thiourea (TU) is widely used in the electrodeposition of metals as a brightener or levelling agent, and also as a complexing additive [1–4], for example, in lixiviation of Au. Several previous studies have been made to investigate the process of adsorption of TU, and the extent and nature of the adsorption reaction [4–7]. It has been found that thiourea is strongly chemisorbed and the adsorption characteristics are similar to those of halide ions [8–10], that is, involving sharing or donation of an e-pair, as also arises in the well known phenomenon of self-assembled monolayer formation of alkane-thiols at Au and Hg.

Gold may be either attacked or passivated [11–14], depending on whether the potential applied is smaller or larger than a critical value, as already observed in galvanostatic experiments reported in 1921 [15] involving transition-time measurements for study of onset of passivation of Au in 0.012 M HCl. The anodic dissolution of Au in acidic solutions of TU, forming Au(I)–TU complex ions was studied by Groenewald [16] who found that, at anodic overpotentials (undefined, cf. [16]) of up to 0.3 V, the dissolution of Au was rapid and approached the maximum diffusion-controlled rate. The exchange current density was stated to be greater than 10^{-6} A cm^{-2}, and dissolution proceeded at 100% efficiency. The dissolution of Au in acidic thiourea solution, together with the oxidation of thiourea on Au, was investigated by Zhang et al. [17]; it was found that at 25 °C and without the presence of an additive, formamidine disulphide (FD), Au did not dissolve when the potential was scanned rapidly. The process of Au dissolution was regarded as possibly indicating a slow heterogeneous step which could be accelerated by FD. Okido et al. [18] investigated the anodic dissolution of Au in alkaline solutions of TU, thiosulfate and sulfite. They concluded that both the solution composition and electrode potential affect the Au dissolution rate and its current efficiency which was only between 10% and 20% in this case.

The redox reaction describing the dissolution of gold in, or its deposition from, acidic thiourea solution is, according to [19]:

$$\mathrm{Au}\ (\mathrm{SC(NH_2)_2^+}) + \mathrm{e^-} = \mathrm{Au} + 2\,\mathrm{SC(NH_2)_2} \qquad (1)$$

and the standard reduction potential was measured as 0.38 V at 25°C. The anodic oxidation of thiourea itself requires one electron per thiourea molecule to yield formamidine disulphide [20]. This couple was considered reversible on platinum [21], with a reduction potential $E^\circ = 0.420$ V.

At the molecular level, the mechanism of facilitation of anodic dissolution of Au by TU remains obscure. Two possibilities are: (a) Au dissolves as monovalent cations, Au^+, which are complexed immediately by TU forming the complex cation $[Au(TU)_2]^+$ (Equation 1) in the double-layer interface (an *ec* mechanism); alternatively, (b) since TU is already chemisorbed, the dissolution/complexation process is a coupled reaction proceeding in a single step at the surface. We believe the latter process is probably the preferred mechanism.

In recent years, the electrochemical quartz-crystal nanobalance (EQCN) has become a common and sensitive tool for the study of electrochemical processes in which mass accumulation (or deficit, as in corrosion) on the electrode is involved [22–25].

Use of the EQCN provides the opportunity for sensitively determining mass changes on an Au electrode surface, deposited on an AT-cut quartz crystal, that arise from change of the oscillation frequency of thin quartz films exhibiting elastic behaviour [26]. The conversion of frequency change (Δf) to mass changes (Δm) during dissolution experiments is possible through the Sauerbrey equation [27]:

$$\Delta m = -\left(\frac{\sqrt{\rho_q \mu_q}}{2nf_0^2}\right)\Delta f = -\left(\frac{N\rho_q}{f_0^2}\right)\Delta f = -C_f \Delta f \qquad (2)$$

where f_0 is the resonant frequency of the quartz-crystal resonator (in our case ~8.94 MHz in air). ρ_q the density of quartz (2.648 g cm^{-3}) [28], μ_q the shear modulus of the quartz (2.947×10^{11} g cm^{-1} s^{-2}), n an harmonic number (for the first harmonic, $n = 1$), N is a frequency parameter (1.67×10^5 Hz cm^{-1}), and C_f is the calibration factor (cf. [29]) for the crystal employed for the measurement. However, limitations to the direct interpretation of measured coupled oscillation frequencies, Δf, in terms of mass changes have been recognized by Tsionsky and Gileadi [30] and well discussed by Hepel [31].

The importance of this electroanalytical tool lies in the possibility of simultaneously measuring *in situ* the mass balance and, by means of CV, the associated extent of passage of charge (q) involved in electrochemical processes, which enables calculation of the effective equivalent weight of the surface species adsorbed on the electrode, or the weight of Au metal dissolved as a function of faradaic charge passed.

Moreover, a comparison with the simultaneously recorded current against time data, using conventional electrochemical procedures, can provide quantitative information on the mechanism involved of the surface process(es) and related evaluation of the efficiency of electrochemical metal deposition or dissolution processes, eliminating interference by non-faradaic currents, which often cannot be achieved by simple electrochemi cal techniques.

While various significant papers on dissolution of Au, facilitated by TU, have been published (as cited above), the aims of the present paper are to provide more quantitative information on this process, especially by means of complementary use of the EQCN technique with regular electrochemical transient procedures such as cyclic voltammetry, chronopotentiometry and chronoamperometry.

2. Experimental details

2.1 *Materials*

$HClO_4$ solution was prepared from SeaStar $HClO_4$ diluted with Barnstead Nanopure water (18 MΩ cm). Thiourea solutions were prepared from the research grade, >99% (Aldrich Chem.) chemical. Well-known procedures for high-purity experimentation, as detailed elsewhere [32], were employed in this work. Electrodes were made from 0.5 mm diameter Aesar Puratronic Au wire (99.99%) sealed in soft glass tubes. EQCN Au-coated quartz crystals were as commercially available. The geometric areas for the gold wire and EQCN Au-coated quartz crystal electrode are 0.39 and 0.20 cm^2, respectively.

2.2. *Electrode areas and roughness factors*

Real specific areas of the Au wire and Au-coated EQCN crystal electrode were determined by the method of Burshtein et al. [33], based on voltammetric evaluation of anodic charge for deposition of O species up to the characteristic 'Burshtein minimum' in the CV current-response curves. This is assumed [33] to the correspond to monolayer formation of O species in the surface oxidation of Au. For Au, this procedure provides the best equivalent to that of determination of UPD H converage at Pt for real area determination. The Burshtein procedure was also employed to check any real-area changes that might arise in the course of TU-assisted dissolution of Au. (Section 3.2).

2.3. *Instrumentation*

Details of the apparatus used in the EQCN experiments have been described previously e.g., [10]. Briefly, the planar AT-quartz crystals used had a fundamental frequency of 8.94 MHz in air (it drops to ~8.90 MHz when the crystal is in contact with electrolytes). Both sides of the crystal surface bore a thin deposit of Au about 300 nm in thickness. The electrodes had a flat surface, little roughness and exhibited no effect associated with the cell geometry that could affect the crystal response. The Au plate working quartz electrode was mounted in a specifically designed Teflon™ holder [10]. The electrochemical cell and the latter quartz-crystal holder have been described previously [10]. The electrode was cleaned with ethanol followed by brief immersion in 1:3 (v/v) H_2O_2 + H_2SO_4 and followed

by rinsing with Milli-Q water. A home-built Faraday cage was used to minimize electronic noise.

A reversible hydrogen electrode (RHE) was used as the reference electrode and a Pt sheet (Aesar, 99.99%) as the counter electrode. For characterization of mass-transfer effects in the observed dissolution of Au, a Pine Instruments Co. (Grove City, PA) rotating-disc Au electrode assembly was used.

Ultrahigh purity Ar was passed through the working electrode compartment to sustain an inert gas environment. Each new Au electrode was cycled at least for 500 times between 0.05 and 1.70 V vs RHE, in order to electrochemically clean and release any stress from the near-surface region [32, 34]. The quality of the Au electrode and cleanliness of electrolyte were verified by recording CV profiles over the 0.05–1.70 V vs RHE range and comparing the response profiles with those accepted in the literature for clean (polycrystalline) Au surfaces.

2.4. *Addition of thiourea*

EQCN and CV experiments were first conducted over a wide range of TU concentrations in order to establish conditions for observation of onset of Au dissolution. An all-glass micrometer burette (Gilmont Instruments), with an accuracy of 0.002 mL, was used to inject controlled volumes of a standard, dilute TU solution into the anode compartment containing an initially known volume of the supporting electrolyte. Each EQCN frequency change and corresponding CV was recorded 360 s after addition of the TU with stirring by bubbling with the Ar gas.

2.5. *Stability of the system*

The stability of the EQCN system was examined by cycling the potential in the range 0.05–1.7 V vs RHE in 0.5 M $HClO_4$. Sixty cyclic voltammograms recorded at 50 mV s^{-1} over a potential range of 0.05 to 1.70 V during one hour showed no systemetric drift, and the anodic and cathodic response changes of frequency in each successive cycle were reproducible to better than 1 Hz. The shift of response frequency in 1 h cycling was about 0.5 Hz and is thus negligible on the time scale of these $\Delta f/t$ curves, indicating that a frequency change well below that for the monolayer level can be measured accurately, without significant drifts.

2.6. *Calibration constant*

The calibration constant, C_f, (Equation 2) was determined as 5.60 ng cm^{-2} Hz^{-1}, as evaluated in [29] and treated in [31, 35, 36].

3. Results and discussion

3.1. *Effect of thiourea on the cyclic voltammograms*

Figure 1 shows a series of cyclic voltammograms (CVs) recorded for an Au electrode in 0.5 M $HClO_4$ solution in the presence of TU at concentrations of (a) 0 (b) 5×10^{-5} (c) 1×10^{-4} and (d) 1×10^{-3} M in the potential range 0.05–1.70 V vs RHE, respectively, according to the annotations of Figure 1. An anodic current peak at a potential at about 1.32 V vs RHE on the positive-going sweep, and a cathodic current peak at about 1.17 V vs

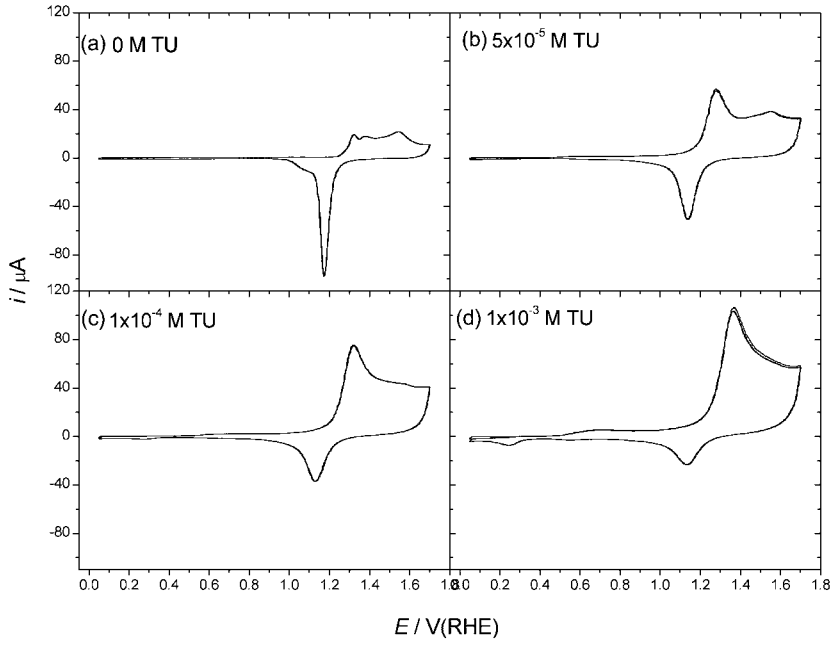

Fig. 1. CVs for a gold electrode obtained in 0.5 M $HClO_4$ solution containing increasing concentrations of thiourea (a) 0, (b) 5×10^{-5} M, (c) 1×10^{-4} M, (d) 1×10^{-3} M cycled over the potential range 0.05 to 1.7 V vs RHE, and at a sweep rate of 50 mV s^{-1}.

RHE in the negative-going sweep, were observed corresponding, respectively, to the growth of the Au oxide and its reduction on the electrode surface in 0.5 M $HClO_4$ solution in the absence of TU (Figure 1(a)) [37, 38]. When the concentration of TU was below 10^{-6} M, no change is detectable for both the peak at about 1.32 V and that at 1.17 V but, as the concentrations of TU exceeded 10^{-6} M, the peak at 1.32 V became gradually shifted to more positive values, while charge for the peak for reduction of anodically-grown oxide became smaller. The difference is attributable to the adsorption of TU on the Au electrode surface that inhibits formation of the oxide over this potential region. However, as the TU concentration becomes greater than 3×10^{-5} M, a new peak was observed at about 1.27 V; the electrochemical reaction involved is considered to be the oxidation of TU to FD [17] represented, as an overall reaction as (cf. [21]), by

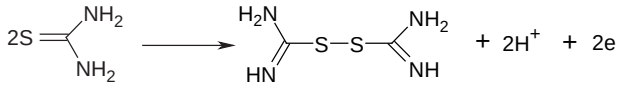

(3)

A two-step mechanism has been suggested by Reddy and Krishnan [21] for the oxidation of thiourea in which the tautomeric form of TU (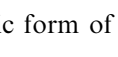) is first oxidized to a TU free-radical on S, followed by the combination of two such radicals to form FD, as in Equation 3.

As the concentration of TU becomes greater than 10^{-4} M, the CVs change dramatically (Figure 1(c) and (d)): an anodic current peak appears at about 0.64 V vs RHE and increases with increasing TU concentration. In addition to the cathodic peak at 1.17 V vs RHE, which is due to the reduction of oxide previously anodically formed on the electrode, a new cathodic peak becomes observable at about 0.25 V vs RHE in the negative–going sweep. Groenewald [16] studied the electrochemical reaction of an acidified TU solution on an Au electrode. An oxidation peak, the potential of which corresponds to that of the peak at 0.64 V in Figure 1(d), was shown to be due to the dissolution of Au with a current efficiency of 100%. The electrode reaction was thought to be as shown in Equation 1. It is interesting to note that the potential for Au dissolution is about 600 mV more negative than that observed in the presence of Br^- or Cl^- (1.20 V vs RHE for Br^- and 1.39 V vs RHE for Cl^-) [10], demonstrating that Au dissolution is easier in the presence of TU, probably due to complexation of resulting Au ions with the TU.

The peak potential for oxidation of TU at an Au electrode is 1.27 V vs RHE, totally different from that at Pt [17, 39]. Thus, it was found for Pt in related, unpublished work that an anodic current peak arises at about 0.65 V vs RHE and a cathodic one at about 0.33 V vs RHE during the positive-going and the negative-going sweep, respectively. Pt being a more stable metal than Au (enthalpy of atomization 200 kJ mol^{-1} greater than for Au) has less tendency for dissolution in the presence of TU. Au, on the contrary, becomes dissolved in the presence of TU which shifts the potential for oxidation of TU to a more positive value on account of the strong chemisorption of TU on the Au surface coupled with complexation upon dissolution. When a TU molecule becomes adsorbed in the double layer, replacing one or more water molecules, it is assumed [5] to adsorb in an orientation normal to the Au surface over a wide range of potential, with the =S atom contacting the Au surface and with the $-NH_2$ groups hydrogen-bonded to water molecules on the electrolyte side of the double-layer.

3.2. *EQCN characterization of the Au-coated crystal electrode in the presence of thiourea*

Figure 2 shows (a) a progressive sequence of the CVs, recorded one after the other and (b) the corresponding sequence of cyclic EQCN frequency changes for the Au-coated crystal electrode recorded at a sweep rate of 50 mV s^{-1} over the potential range 0.05 to 1.05 V in 0.5 M $HClO_4$ solution containing 3×10^{-3} M TU. An anodic current peak at about 0.675 V vs RHE is observed in the positive-going potential sweep and becomes shifted to more negative potential (0.630 V vs RHE) during the following sweep. Cathodic current peaks at about 0.436 and 0.336 V vs RHE arise in the negative-going potential sweep. Similar voltammetric behaviour was observed in [17]. The cathodic peak current at 0.436 V vs RHE is due to the reduction of a gold–thiourea complex formed during the anodic reaction, and the current peak at 0.337 V vs RHE is due to the reduction of FD formed according to Equation 3.

The Δf increases rapidly as soon as charge is passed at 0.50 V vs RHE. However, once the potential becomes more positive than that of the anodic current peak, Δf only increases more slowly. Thus, the net frequency increase is 560 Hz for the first cycle but becomes smaller in the following sweep. The value of Δf at the completion of a given single CV cycle is 365 Hz, that is, a value more positive than that at the beginning of that cycle, thus corresponding to the electrode becoming progressively 'lighter'. This behaviour is quite different from that in thiourea-free $HClO_4$ solution where no net progression of Δf was found during a multiple sequence of potential cycles in distinction to the actual progression of changes of Δf on cycling with TU present as seen in Figure 2(b) and in [40]. This indicates that Au is being continuously dissolved during the potential cycling in the presence of thiourea but is not fully redeposited in the following negative-going potential scan. Direct evidence for this was provided by u.v.–vis. spectrometry of a solution in which an Au electrode was held at 0.65 V vs RHE for various times: the absorption for the band at 235 nm for free TU decreases with increasing time. The associated decrease in concentration of TU is

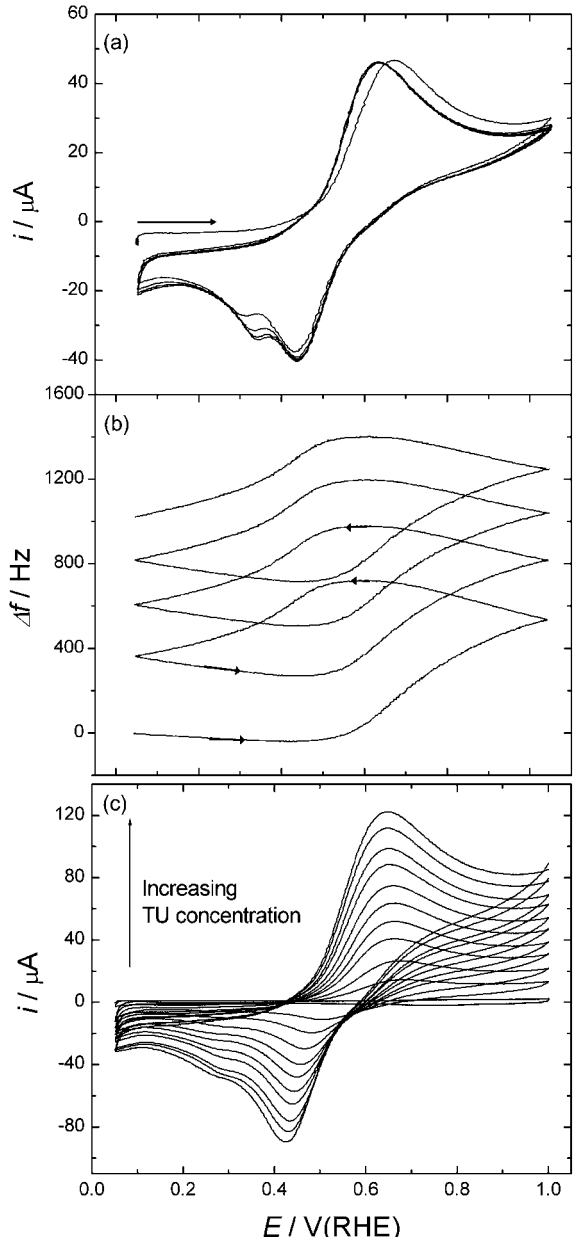

Fig. 2. CVs (a) and simultaneously recorded frequency responses (b) of an Au-coated EQCN crystal electrode in 0.5 M $HClO_4$ in the presence of 3×10^{-3} M thiourea. Sweep-rate 50 mV s^{-1}; potential range 0.05–1.05 V vs RHE. (c) CVs of an Au electrode in the presence of various concentrations of TU in the range 2.5×10^{-4}–2.5×10^{-3} M.

due to its complexation with Au(I), which was produced during the anodic Au dissolution.

The anodic dissolution, especially as indicated by the EQCN results (e.g., Figure 6), raises the question whether the EQCN Au surface becomes roughened as a result of such dissolution, assisted by TU, with a consequent possible substantial change of apparent mass response. Thus, Schumacher et al. [41] have found that Au electrode surfaces that have become roughened by strong anodic surface-oxide film formation, can suffer 'substantial' apparent mass increases due to confinements of electrolyte solution within microscopic pockets in the oxidized surface.

In our experiments, dissolution occurs at potentials substantially lower than those for onset of surface oxide formation due to the presence of TU but roughening could occur in the dissolution process for different reasons, leading to a solution entrainment contribution in the measured EQCN frequency change (cf. [41]). Experiments were therefore conducted by the voltammetric charge procedure of Burshtein et al. ([33] and Section 2.2) to determine if significant surface roughening took place due to dissolution assisted by the presence of TU. The results for the roughness factors, R, were as follows: before dissolution, $R = 1.60 \pm 0.02$; after dissolution in the presence of TU, $R = 1.63 \pm 0.02$, that is, there is no change within the limits of experimental error. Thus, any roughening effects are quite insufficient to lead to any enormous mass changes due to entrainment, especially since oxide-film formation [41] was not involved. Also the entrainment effect was not one of the significant effects, other than absolute mass changes, envisaged by Tsionisky et al. [30] in their analysis of possible factors in processing EQCN electrode behaviour.

Figure 2(c) shows a series of CVs recorded for an Au electrode in 0.5 M $HClO_4$ solution with gradual additions of TU. The anodic peak for Au dissolution slightly shifts negatively at first, then remains constant. However, the cathodic peak for Au-complex redeposition continuously shifts to less positive potential. There is about 80 mV change of potential of cathodic peak but only about 15 mV for the anodic peak as concentration of TU is increased from 2.5×10^{-4} to 2.5×10^{-3} M. Both anodic and cathodic peak currents increase as the concentration of TU is increased.

The correlation between voltammetric and mass change behaviour can be verified by calculating the equivalent current involved in this process through numerical differentiation of mass changes with respect to time. The faradaic current corresponding to the Au dissolution process can be calculated from the derivative, $d(\Delta f)/dt$, of the EQCN frequency change, after conversion to mass change (Equation 2), for a supposed $1e^-$ charge transfer process (Equation 1). The results are shown in Figure 3, Curve (···) shows the two complete CV cycles for the Au-coated EQCN crystal electrode in 3×10^{-3} M TU. Curve (——) is the equivalent current for Au dissolution, calculated from mass change [42]. Figure 3 shows that the calculated current is consistent with the recorded voltammetric current behaviour at both the anodic and the cathodic current peaks, demonstrating that the dissolution process occurs faradaically according to Equation 1.

The Au could be dissolved through either a $3e^-$ or/ $1e^-$ transfer process. The apparent molar masses for these two processes are 65.7 and 197 g $(mol\ e^-)^{-1}$, respectively. The apparent molar masses of the dissolved species can be obtained from an analysis of the slope of the Δm against q profile obtained complementarily from the CV and EQCN experiments [43, 44]. The molar mass of the dissolved species in the anodic process was estimated to

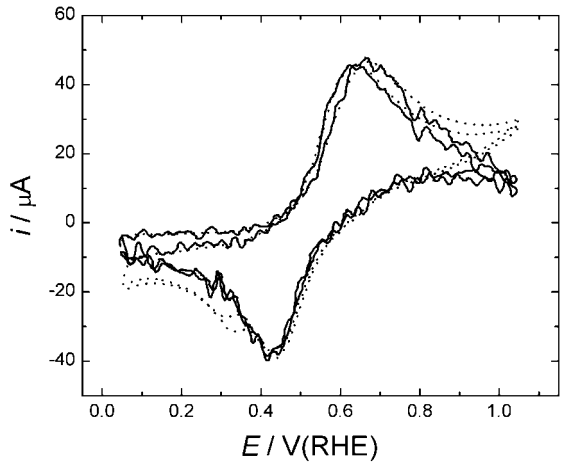

Fig. 3. Measured (···) and calculated (——) voltammograms for an Au-coated crystal electrode in 0.5 M $HClO_4$ in the presence of 3×10^{-3} M thiourea.

be 190.2 g (mol e^-)$^{-1}$, which is in consistent only with the $1e^-$ transfer process rather than the $3e^-$ transfer.

3.3. *Effect of variation of sweep-rate and of positive potential limit on the process involved*

Figure 4(a) shows the CVs for the Au disc electrode in 0.5 M $HClO_4$ solution containing 5×10^{-3} M TU, as the sweep-rate was varied from 10 to 100 mV s^{-1}, cycled over the potential range 0.05 to 1.0 V vs RHE. Both the anodic current at about 0.64 V vs RHE and cathodic current at about 0.44 V vs RHE increase with sweep-rate. The cathodic peak potential is shifted negatively with sweep-rate, as is usually observed [45]. The difference between the anodic and cathodic peak potentials is about 0.20 V for a sweep-rate (v) of 10 mV s^{-1} and increases slightly with increase of v. The anodic peak currents (i) at about 0.64 V vs RHE and those for cathodic peak at about 0.44 V vs RHE are plotted as a function of square-root of v in Figure 4(b), which shows a clear linear dependence of i on $v^{1/2}$ indicating a diffusion-controlled process for Au dissolution and redeposition in the presence of TU. The same result is obtained from our impedance measurements (Figure 5). The impedance spectra, based on the standard 5 mV potential modulation, were recorded in 0.5 M $HClO_4$ containing 3×10^{-3} M TU over a frequency range of 100 kHz to 0.1 Hz. As can be seen from Figure 5, both kinetically-controlled (semicircular) and diffusion-controlled (linear, minus-unity slope in the Nyquist diagram) behaviours are displayed. In the high-frequency region, the dissolution is kinetically-controlled, but, over the low-frequency region, a linear relationship between $-Z''$ and Z' (−45° phase-angle) indicates that the process is diffusion-controlled.

Δf values decrease dramatically with increasing v: Δf is 1221 Hz for $v = 10$ mV s^{-1}, but is only 383 Hz at 80 mV s^{-1}. The lower the sweep-rate, the larger is the mass change, because longer periods of time are provided in a slow than in a fast sweep, allowing greater extent of Au dissolution to arise.

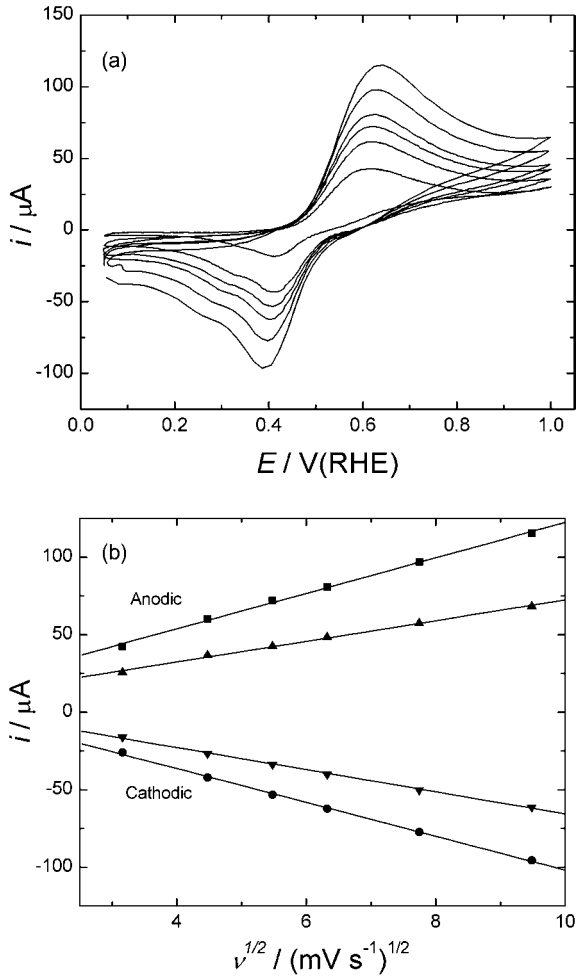

Fig. 4. (a) CVs for an Au disc electrode obtained at various sweep-rates in 0.5 M $HClO_4$ solution in the presence of thiourea. Sweep rates: 10, 20, 30, 40, 60, and 90 mV s^{-1}. (b) anodic and cathodic peak currents plotted as a function of the square-root of sweep-rate: (■) 3×10^{-3} M; (▲) 1×10^{-3} M; (▼) 1×10^{-3} M and (●) 3×10^{-3} M.

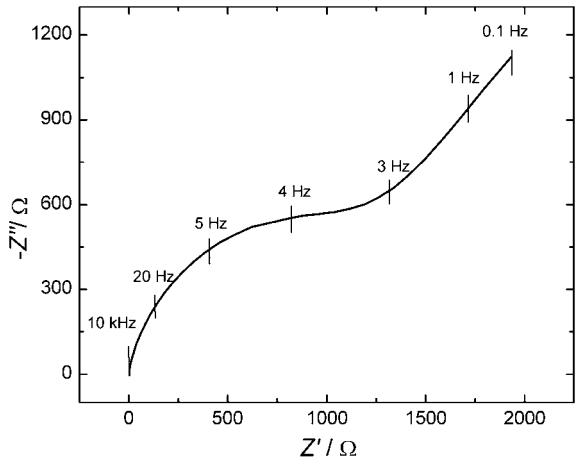

Fig. 5. Impedance plane plots for an Au electrode obtained in 0.5 M $HClO_4$ containing 3×10^{-3} M thiourea. Frequency range 0.1 Hz–100 kHz.

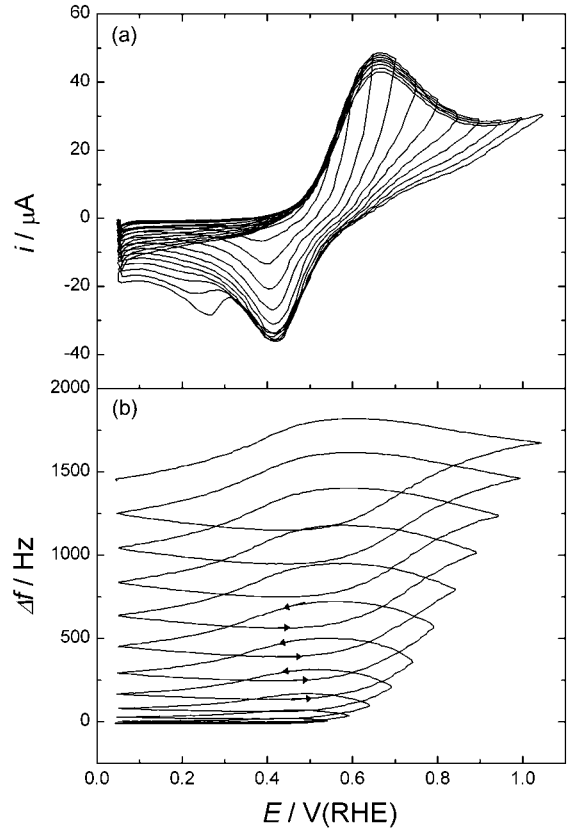

Fig. 6. CVs (a) and simultaneously recorded frequency responses (b) for the Au-coated EQCN crystal electrode obtained for successive increases of positive reversal limit of the potential sweep between 0.4 and 1.0 V vs RHE; sweep rate 50 mV s^{-1}; 3×10^{-3} M thiourea in 0.5 M $HClO_4$.

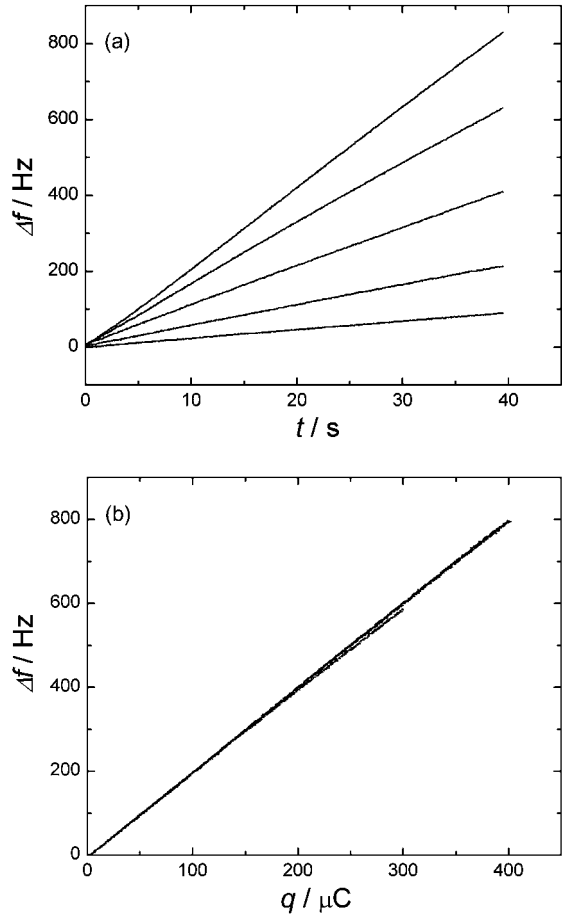

Fig. 7. (a) Frequency change against time responses for the Au-coated electrode in 0.5 M aqueous $HClO_4$ + 3×10^{-3} M thiourea at various constant current densities. $i = 1$, 2.5, 5.0, 7.5 and 10 μA. (b) The relationship between mass change (Δm) and anodic charge passed during the dissolution.

Obviously, these results are totally different from those obtained in [17], where it was found that below 20 mV s^{-1} the peak current increases with increasing sweep-rate. Above the 20 mV s^{-1}, however, the peak current started to drop. The reason for this difference is probably that a relatively high concentration of TU was used (0.1 M) coupled with rotation of the electrode in their experiments.

Figure 6 shows the potential dependence of current and the corresponding Δf behaviour observed during potential cycling between +0.05 V and various positive potential limits in 0.5 M $HClO_4$ solution in the presence of TU. No significant change of either current or Δf were observed in the potential range 0.05 to 0.5 V vs RHE. However, as the potential was scanned beyond the limit 0.5 V, Δf increases corresponding to the anodic currents passing in the CV over the potential range 0.5 to 0.65 V in the positive-going sweep. This is attributed to the diffusion-controlled dissolution of Au as discussed in Section 3.3. If the upper potential limit for cycling was less than 0.9 V vs RHE, only one cathodic current peak is observed at about 0.43 V vs RHE; and becomes slightly shifted in the positive direction as the positive reversal potential limit is increased. When the upper potential limit is beyond 0.9 V vs RHE, a second cathodic current peak is observed at about 0.28 V vs RHE and is due to the reduction of FD which had been formed in the positive-going potential sweep.

3.4. *Chronopotentiometry experiments*

This method is based on application of a constant-current (i) pulse with recording of the resulting potential response and frequency changes (Δf) against time (t). Constant currents, having values between 1 and 10 μA were applied for a period 40 s and the corresponding EQCN frequency responses were recorded as a function of time (Figure 7). The resulting frequency change against time ($\Delta f/t$) relations are linear with no significant deviations.

The theoretical value of the ratio of mass to charge for the process of $1e^-$ dissolution of Au in the presence of TU is 197 g (mole e^-)$^{-1}$. The molar mass of dissolved species obtained from the slope of the mass change against charge relation for the Au dissolution processes is 215 $\pm$ 8 g (mol e^-)$^{-1}$ (Figure 7(b)). This value is only slightly greater ($\sim$9%) than the theoretical value (197, for $1e^-$ transfer), suggesting a simple electrochemical process in which all mass variations were directly associated with the dissolution of Au.

3.5. *Potentiostatic experiments*

Analyses of dissolution processes, in relation to their kinetic characteristics, are frequently based on the measurements and interpretation of current-transient responses during a potential step applied to the working electrode in chronoamperometric experiments. This technique is one of the most appropriate for investigating of nucleation and dissolution processes because it allows the driving forces for these processes to be properly controlled through the use of constant electrode potential as the perturbation.

In this series of experiments, the potential was stepped from an initial value $E_i = 0.30$ V (where no Au dissolution of the electrode takes place) to second values of E taken between 0.50 and 0.70 V vs RHE in successive intervals of 50 mV. The duration of each step was 95 s, then the potential was stepped back to its initial value. As shown in Figure 8(a) electrolysis for 95 s at 0.65 V caused a frequency increase of 1611 Hz that is equivalent to a mass decrease of 1.9 μg of Au. The corresponding charge passed is 0.95 mC (Figure 8(b)). The theoretical charge calculated from Faraday's law for the dissolution of Au to Au(I) is 0.89 mC, thus, the current efficiency is about 93% for gold dissolution in the present medium.

For the redeposition process, only a much smaller charge (0.56 mC) is required; the corresponding frequency change was also recorded (846 Hz). Similar behaviours were observed at other step potentials. The charge for the process of Au redeposition from the Au(I)-complex species is always smaller than that for the dissolution process owing to their escape into the bulk solution. Furthermore, the frequency change can be plotted against the charge passed, as in Figure 8(c), giving the estimated apparent molar equivalent weights for the dissolution and redeposition processes as 191.3 and 185.8 g (mol e^-)$^{-1}$, respectively [44]. Both values are only slightly smaller than the theoretical value (197 g (mol e^-)$^{-1}$), which confirms again that the dissolution and redeposition processes take place via $1e^-$ transfer processes.

The transient i/t function for a planar electrode in a chronoamperometry experiment is given by Cottrell's equation [46]:

$$i = \frac{nFAD_o^{1/2}C_o^{\infty}}{\pi t^{1/2}} \tag{4}$$

where D_o, C_o^{∞} are the diffusion coefficient and bulk concentration, respectively, of the diffusing species. Integration of Equation 4 enables the cumulative

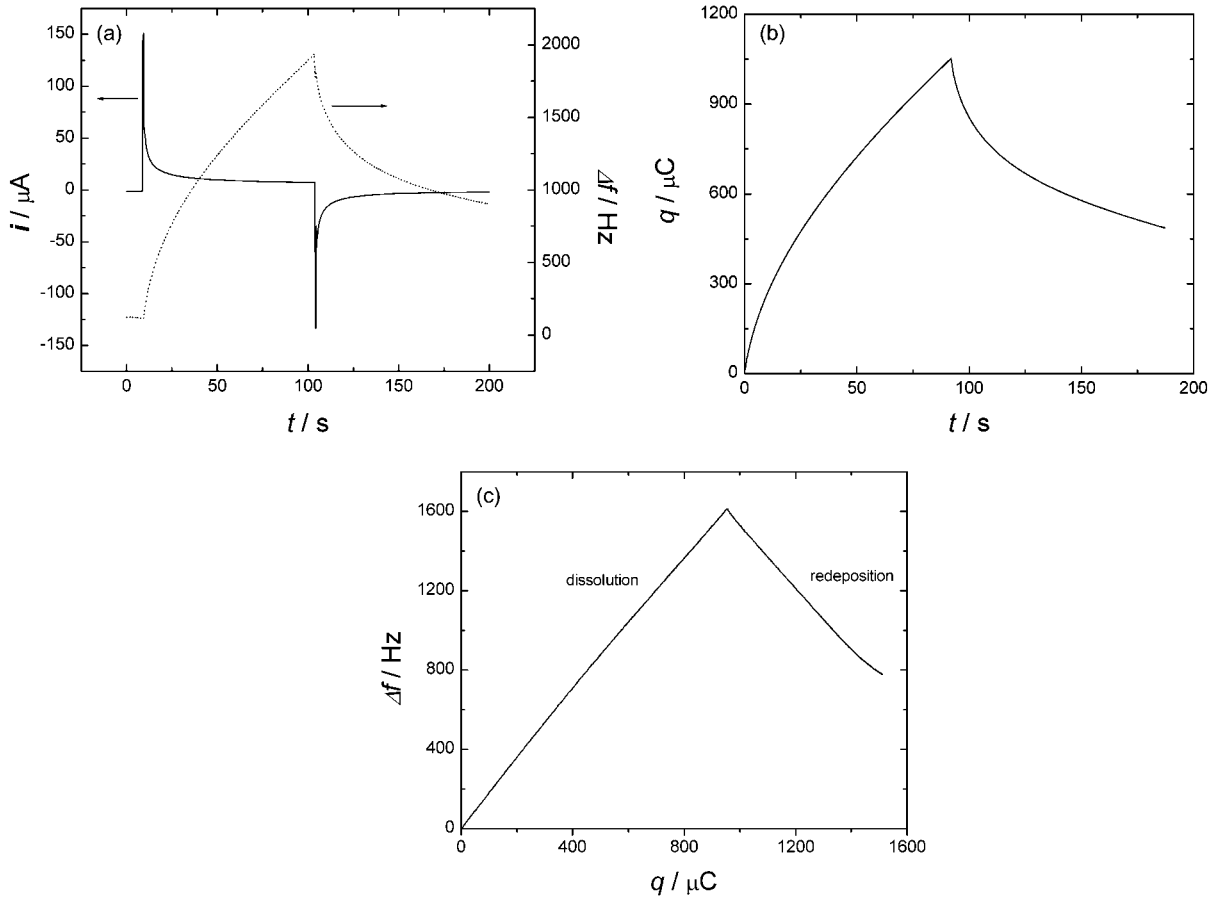

Fig. 8. (a) Time-dependence of transient current and frequency change recorded simultaneously as potential was stepped from 0.3 to 0.65 V vs RHE in 0.5 M $HClO_4$ containing 3×10^{-3} M thiourea; (b) charge change and (c) a plot of frequency change against charge passed.

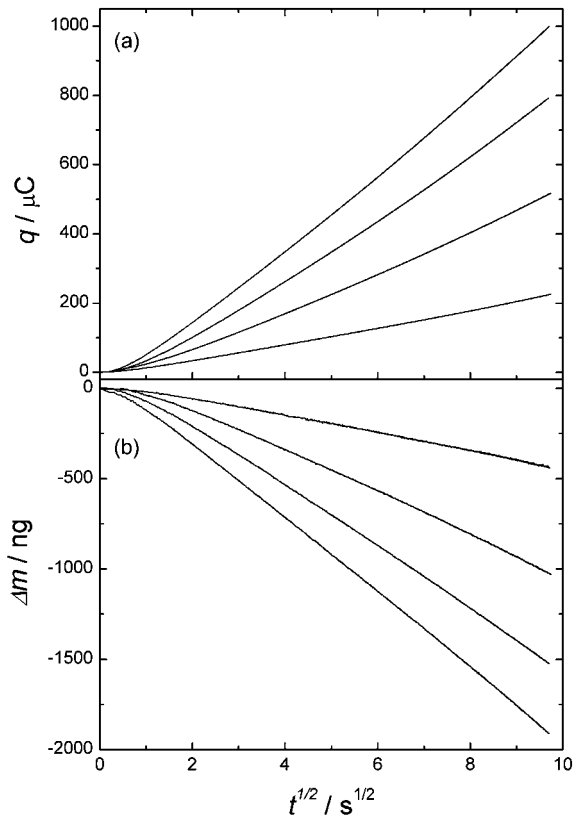

Fig. 9. Time-dependence of anodic charge (a) and mass change (b) obtained following potential steps from 0.30 V to 0.50, 0.55, 0.60, 0.65 V vs RHE in 0.5 M $HClO_4$ containing 3×10^{-3} M thiourea.

charge, q, for reduction of the diffusing reactant to be linearly related to $t^{1/2}$. Then, from Faraday's law, $\Delta m = qM/nF$, the relationship between Δm and t, equivalent to Cottrell's equation, is obtained:

$$\Delta m = \frac{2D_o^{1/2}C_o^{\infty}t^{1/2}M}{\pi^{1/2}} \tag{5}$$

Figure 9a shows the relationship between anodic charge, q, measured at Au, and $t^{1/2}$, following potential steps to various constant final potentials (0.50, 0.55, 0.60, 0.65 V vs RHE). The charge, q, increases almost linearly with $t^{1/2}$, in the range 0.5–9.7 $s^{1/2}$. The slope of the curve also increases with increase of the step potential, ΔE.

Experimental mass transients can also be simultaneously recorded in the potentiostatic experiments, results of which are shown in Figure 9(b). Δm decreases linearly with $t^{1/2}$, with the slope of the $\Delta m/t^{1/2}$ relation also increasing slightly as the step potential is increased to larger values. The resulting linear relationship between Δm and $t^{1/2}$ is consistent with theoretical expectations (Equation 5). The linear relationships between charge, q, or Δm and $t^{1/2}$ clearly indicate that the dissolution process is diffusion-controlled and limited by the mass transport of TU towards, or of $Au[TU]_2^+$ (Equation 1), away from the electrode.

3.6. *Study of Au dissolution in solutions containing thiourea, using a RDE*

The rotating-disc electrode technique was used to study anodic dissolution of Au in the presence of TU in 0.5 M $HClO_4$. In the cyclic voltammogram, an anodic peak arises for dissolution of Au at a potential of about 620 mV. The EQCN results in Section 3.2 showed that Au dissolution occurs in the presence of TU according to Equation 1. The current for that process, under kinetic-control, can be represented by a Butler–Volmer type of equation, as applied by Alodan and Smyrl [6] for copper dissolution, taking into account the backward and forward direction of process 1:

$$\frac{i}{F} = k_a[TU]_s\, e^{\alpha_a FE/RT} - k_c[Au(TU)_2^+]\, e^{-\alpha_c FE/RT} \tag{6}$$

where $[TU]_s$ is the surface concentration of TU. E represents a nonequilibrium electrode potential, i is the net current, and α_a and α_c are the anodic and cathodic transfer coefficient, respectively.

Process 1 will tend to be kinetically controlled at relatively low values of E (first term on the right in Equation 6), while, when E is sufficiently high, diffusion will control the anodic current. Under kinetic control, at low value of E and/or at infinite rotation rate in a rotating-disc experiment, an anodic Tafel slope from Equation 6 will arise having a value:

$$\frac{dE}{d(\log i_\infty)} = \frac{2.303RT}{\alpha_a F} = 120\,\text{mV decade}^{-1} \text{ at } 298\,\text{K} \tag{7}$$

for $\alpha_a = 0.5$, say. On the other hand, at sufficiently high positive potential at a rotating-disc electrode, a limiting, diffusion-controlled current, i_{lim}, will arise for a bulk concentration, $[TU]_b$, corresponding to the Levich equation:

$$i_{lim} = \frac{FD^{1/3}\omega^{1/2}[TU]_b}{1.611\nu^{1/6}} \tag{8}$$

A plot of i_{lim} against $\omega^{1/2}$ should then give a straight line with a slope proportional to the concentration of TU.

Figure 10 shows the effect of rate of rotation, ω, on the i/E curves obtained in 0.5 M $HClO_4$ containing 5×10^{-3} M TU at a sweep rate of 20 mV s^{-1}, for a range of ω between 0 and 600 rpm. Without rotation, an anodic current peak arises at about 0.62 V vs RHE and a cathodic one at about 0.42 V vs RHE; however, with rotation, the cathodic current disappears because the anodically formed, soluble $Au(TU)_2^+$ species are spun-off into bulk solution and are thus not recovered through redeposition in the conjugate negative-going sweep. As already seen in Figure 10, passivation occurs during gold dissolution at the RDE as was observed by Zhang et al. [17] who found that the voltammetric

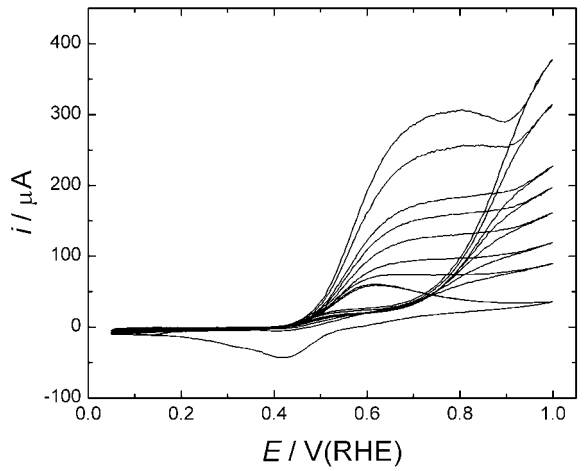

Fig. 10. Cyclic voltammograms for the rotating Au disc electrode recorded at various rotation rates in 0.5 M $HClO_4$ containing 3×10^{-3} M thiourea. Rotation rates 0, 25, 50, 100, 150, 200, 400, and 600 rpm. Sweep rate: 20 mV s^{-1}.

sweep-rate has some effect on the passivation process. For a low v of 1 mV s^{-1}, the voltammograms are similar in both positive-going and negative-going directions of sweep, demonstrating that the passive film is dissolving. However, a greater sweep-rate (10 mV s^{-1}) does not provide sufficient time for the passive film to be dissolved, so little current is observed in the negative-going, redeposition sweep.

A linear relationship is observed between the limiting current and the square-root of the rotation rate for different concentrations of TU, as expected from Equation 8. The slopes of such linear relationships can be plotted against the concentration of TU, enabling the diffusion coefficient of TU to be derived from the slope of such a plot. From the observed slope of 3.36 ± 0.04, the diffusion coefficient of TU was calculated to be $8.6(\pm 0.1) \times 10^{-6}$ cm^2 s^{-1}, which is close to the literature values [47, 48].

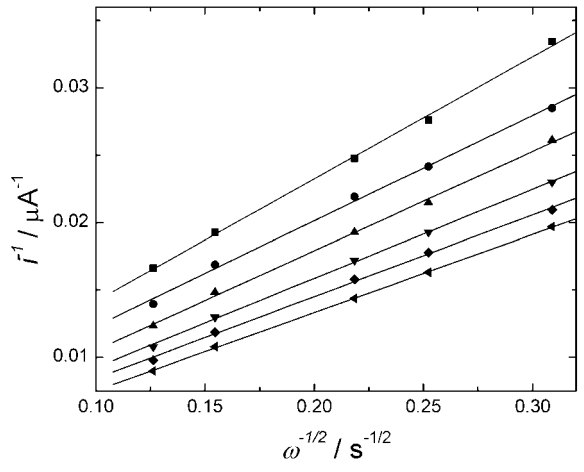

Fig. 11. Plots of i against $\omega^{-1/2}$ for the RDE experiment in 0.5 M $HClO_4$ containing 3×10^{-3} M thiourea. Potential is increased from 0.56 to 0.61 V vs RHE with a interval 10 mV.

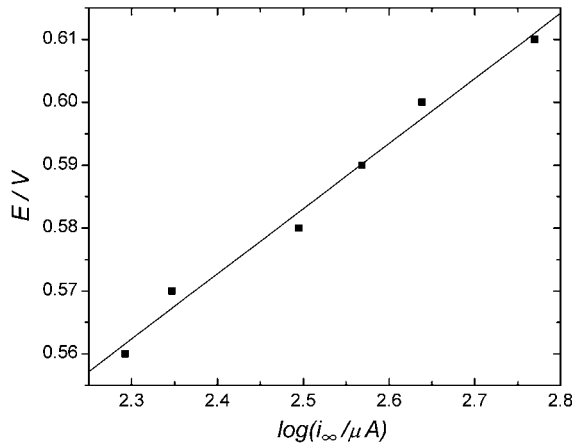

Fig. 12. Plot of the anodic potential against log kinetic current (i_∞), at extrapolated infinite rotation rate (∞) of the Au electrode in 0.5 M $HClO_4$ containing 3×10^{-3} M thiourea.

Figure 11 shows the good linear relationships that are observed between the i^{-1} and $\omega^{-1/2}$ in 0.5 M $HClO_4$ containing 3×10^{-3} M thiourea. However, the lines are not quite parallel, as required for ideal Koutečky–Levich plots; such deviations probably indicate some small, but significant, deviations from pure diffusion control. Similar behaviour has been demonstrated [49] where examples have been shown, exhibiting lines of different slope (e.g., for Zn dissolution). The extrapolated currents at infinite rotation rate, i_∞, can be obtained from the intercepts of the straight lines. A resulting plot of the anodic potential against log i_∞ is a straight line (Figure 12) having a slope of 104 mV decade^{-1} which corresponds to an α_a value of 0.57 derived from Equation 7, close to the value of 0.5 for a symmetrical barrier.

4. Conclusions

The anodic dissolution of an Au electrode in aq. $HClO_4$ containing various concentrations of TU was studied using cyclic voltammetry, chronopotentiometry and chronoamperometry, complemented with nanogravimetry using an EQCN. The results clearly indicate that Au becomes dissolved over the potential range 0.45 to 0.65 V vs RHE via a 1e oxidation process in 0.5 M $HClO_4$ solution containing TU. The peak potential for Au dissolution in the presence of TU is about 600 mV less positive than that in the presence of Br^- or Cl^-. The dissolution current calculated from EQCN Δf data is in good agreement with that derived from voltammograms at both their anodic and cathodic current peaks. The oxidation of the TU itself at Au arises at about 0.60 V more positive than that at Pt. The combination of the EQCN mass and the electrochemical charge data provides a useful approach to the understanding of mechanisms of processes involving metal dissolution or deposition, and the possible species involved (e.g., $Au(TU)_2^+$). In particular it further confirms that the

dissolution process arises through a $1e^-$ electron-transfer, coupled with complexation of TU.

Acknowledgement

Grateful acknowledgement is made to the Natural Sciences and Engineering Research Council for support of this work.

References

1. B. Ke, J.J. Hoekstra, B.C. Sison and D. Trivich, *J. Electrochem. Soc.* **106** (1959) 382.
2. Ph. Javet and H.E. Hintermann, *Electrochim. Acta* **14** (1969) 527.
3. E. Dutkiewicz and R. Parsons, *J. Electroanal. Chem.* **11** (1965) 197.
4. F.A. Blomgren and J. O'M Bockris, *Nature*, *London* **186** (1960) 305.
5. H. Wroblowa and M. Green, *Electrochim. Acta* **8** (1963) 679.
6. M. Alodan and W. Smyrl, *Electrochim. Acta* **44** (1998) 299.
7. B. Reents, W. Plieth, V.A. Macagno and G.I. Lacconi, *J. Electroanal. Chem.* **453** (1998) 121.
8. G. Brown, G. Hope, D. Schweinsberg and P. Fredericks, *J. Electroanal. Chem.* **380** (1995) 161.
9. M. Fleischmann, I. Hill and G. Sundholm, *J. Electroanal. Chem.* **157** (1983) 359.
10. M. Tian, W.G. Pell and B.E. Conway, *J. Electroanal. Chem.* **552** (2003) 279.
11. S.H. Cadle and S. Bruckenstein, *J. Electroanal. Chem.* **48** (1973) 325.
12. S.G.D. Shackleford, C. Boxall, S.N. Port and R.J. Taylor, *J. Electroanal. Chem.* **538** (2002) 109.
13. R.P. Frankenthal and D.E. Thompson, *J. Electrochem. Soc.* **129** (1982) 1192.
14. S. Ye, C. Ishibashi, K. Shimazu and K. Uosaki, *J. Electrochem. Soc.* **145** (1998) 1614.
15. Lobry de Bruyn, *Recl. Trav. Chim. Pays Bas* **40** (1921) 53.
16. T. Groenewald, *J. Appl. Electrochem.* **5** (1975) 71.
17. H.G. Zhang, I.M. Ritchie and S.R.L. Brooy, *J. Electrochem. Soc.* **148** (2001) 146.
18. M. Okido, M. Ishikawa and L.Y. Chai, *Trans. Nonferrous Met. Soc. China* **12** (2002) 519.
19. V.P. Kazakov, A.I. Lapsjin, and B.I. Pescheviski, Russ. *J. Inorg. Chem.* **9** (1964) 708.
20. P.W. Preisler and L. Berger, *J. Am. Chem. Soc.* **69** (1947) 322.
21. S.J. Reddy and V.R. Krishnan, *J. Electroanal. Chem.* **27** (1970) 473.
22. S. Bruckenstein, A. Fensore, Z. Li and A.R. Hillman, *J. Electroanal. Chem.* **370** (1994) 189.
23. Y. Mo, Y. Gofer, E. Hwang, Z. Wang and D.A. Scherson, *J. Electroanal. Chem.* **409** (1996) 87.
24. A. Zolfaghari, B.E. Conway and G. Jerkiewicz, *Electrochim. Acta* **47** (2002) 1173.
25. Q. Chi, T. Tatsuma, M. Ozaki, T. Sotomura and N. Oyama, *J. Electrochem. Soc.* **145** (1998) 2369.
26. H. Gomez, R. Henriquez, R. Schrebler, G. Riveros and R. Cordova, *Electrochim. Acta* **46** (2001) 4309.
27. G. Sauerbrey, *Z. Phys.* **155** (1959) 206.
28. O. Melroy, K. Kanazawa, J.B. Gordon and D.A. Buttry, *Langmuir* **2** (1986) 697.
29. G. Vatankhah, J. Lessard, G. Jekiewicz, A. Zolfaghari and B.E. Conway, *Electrochim. Acta* **48** (2003) 1613.
30. V. Tsionsky, L. Daikhin and E. Gileadi, *J. Electrochem. Soc.* **143** (1996) 2240.
31. M. Hepel, *in* A. Wieckowski (Ed.), 'Interfacial Electrochemistry: Theory, Experiment and Application' (Marcel Dekker, New York, 1999), Chapter 34, p. 599.
32. H.A. Kozlowska, *in* J.O'M. Bockris, E. Yeager, B.E. Conway (Eds), 'Comprehensive Treatise of Electrochemistry', Vol. 9 (Plenum Press, New York, 1984), Chapter 2.
33. R.K. Burshtein, M.R. Tarasevich and V.S. Vulinskaya, *Electrokhimiya* **3** (1967) 349.
34. R. Woods, *in* A.J. Bard (Ed.), 'Electroanalytical Chemistry', Vol. 9 (Marcel Dekker, New York, 1976), pp. 1–162.
35. D.A. Buttry, *in* A.J. Bard (Ed.), 'Electroanalytical Chemistry', Vol. 17 (Marcel Dekker, New York, 1991).
36. G. Jekiewicz, G. Vatankhah, A. Zolfaghari and J. Lessard, *Electrochem. Comm.* **1** (1999) 416.
37. J.S. Gordon and D.C. Johnson, *J. Electroanal. Chem.* **365** (1994) 275.
38. S. Bruckenstein and M. Shay, *J. Electroanal. Chem.* **188** (1985) 131.
39. A.E. Bolzan, I.B. Wakenge, R.C. Salvarezza and A.J. Arvia, *J. Electroanal. Chem.* **475** (1999) 181.
40. M. Tian, W.G. Pell and B.E. Conway, *Electrochim. Acta* **48** (2003) 2675.
41. R. Schumacher, G. Borges and K.K. Kanazawa, *Surf. Sci.* **163** (1985) 1621.
42. A.N. Correia, M.C. dos Santos, S.A.S. Machado and L.A. Avaca, *J. Electroanal. Chem.* **547** (2003) 53.
43. M.J. Henderson, E. Bitziou, A.R. Hillman and E. Viel, *J. Electrochem. Soc.* **148** (2001) E105.
44. G.S. Ostrom and D.A. Buttry, *J. Electroanal. Chem.* **256** (1988) 411.
45. H. Angerstein-Kozlowska, B.E. Conway and W.B.A. Sharp, *J. Electroanal. Chem.* **43** (1973) 9.
46. F.G. Cottrell, *Z. Phys. Chem.* **42** (1902) 85.
47. U. Mishra, S. Tripathi and K. Yadava, *J. Electrochem. Soc. India* **38** (1987) 147.
48. J. Kirchnerova and W.C. Purdy, *Anal. Chim. Acta* **123** (1981) 83.
49. Southampton Electrochemistry Group, 'Instrumental Methods in Electrochemistry', (Ellis Horwood, Chichestes, UK, 1985), Chapter 4 (Figures 4.13 and 4.14).